INVITED PAPER

Ambient RF Energy-Harvesting Technologies for Self-Sustainable Standalone Wireless Sensor Platforms

This paper presents various ambient energy-harvesting technologies and investigates their applicability in the development of self-sustaining wireless platforms.

By Sangkil Kim, *Student Member IEEE*, Rushi Vyas, *Member IEEE*, Jo Bito, Kyriaki Niotaki, *Student Member IEEE*, Ana Collado, *Senior Member IEEE*, Apostolos Georgiadis, *Senior Member IEEE*, and Manos M. Tentzeris, *Fellow IEEE*

ABSTRACT | In this paper, various ambient energy-harvesting technologies (solar, thermal, wireless, and piezoelectric) are reviewed in detail and their applicability in the development of self-sustaining wireless platforms is discussed. Specifically, far-field low-power-density energy-harvesting technology is thoroughly investigated and a benchmarking prototype of an embedded microcontroller-enabled sensor platform has been successfully powered by an ambient ultrahigh-frequency (UHF) digital TV signal (512–566 MHz) where a broadcasting antenna is 6.3 km away from the proposed wireless energy-harvesting device. A high-efficiency dual-band ambient energy harvester at 915 MHz and 2.45 GHz and an energy harvester for on-body application at 460 MHz are also presented to verify the capabilities of ambient UHF/RF energy harvesting as an enabling technology for Internet of Things and smart skins applications.

KEYWORDS | Ambient energy harvesting; autonomous sensors; charge pump; digital TV; dual-band rectenna; embedded microcontroller; energy harvesting; power scavenging; radio-frequency (RF) energy harvesting; RF–dc conversion; ultrahigh frequency (UHF); voltage multiplier; wireless power

I. INTRODUCTION

"Green" self-sustainable operation is one of the most important issues in today's low-power electronics for smart environments (Internet of Things, smart skins, smart cities, etc.). Energy-harvesting technologies harnessing energy from ambient power sources, such as vibration, heat, and electromagnetic waves, have recently attracted significant attention, and numerous energy-harvesting systems, including energy-harvesting devices, topologies, and circuitries, have been developed for "zero-power" self-sustainable standalone electronics [1]–[3]. Among the multiple ambient energy sources, the wireless energy-harvesting technology has dramatically grown recently due to prevalence of wireless signals, such as TV, radio, cellular, satellite, and WiFi signals, especially after the early 1990s. The concept of wireless energy harvesting has been raised by Nikola Tesla and Heinrich Hertz: radiate wireless power to free space and convert the wireless power to usable direct

Manuscript received April 29, 2014; revised August 18, 2014; accepted September 8, 2014. Date of publication October 14, 2014; date of current version October 16, 2014. This work was supported by the National Science Foundation (NSF), the New Energy and Industrial Technology Development Organization (NEDO), the Defense Threat Reduction Agency (DTRA), the Spanish Ministry of Economy and Competitiveness and FEDER funds under Project TEC2012-39143, the European Union (EU) Marie Curie FP7-PEOPLE-2009-IAPP 251557, and the COST Action IC1301 "Wireless Power Transmission for Sustainable Electronics (WIPE)."

S. Kim, **J. Bito**, and **M. M. Tentzeris** are with the School of Electrical and Computer Engineering, Georgia Institute of Technology, Atlanta, GA 30332-250 USA (e-mail: ksangkil3@gatech.edu).

R. Vyas was with the School of Electrical and Computer Engineering, Georgia Institute of Technology, Atlanta, GA 30332-250 USA. He is now with the Schulich School of Engineering and the Pipeline Engineering Center (PEC), University of Calgary, Calgary, AB T2N 1N4 Canada.

K. Niotaki, **A. Collado**, and **A. Georgiadis** are with the Centre Tecnològic Telecomunicacions Catalunya (CTTC), Castelldefels, 08860 Spain (e-mail: nkiriaki@gmail.com).

Digital Object Identifier: 10.1109/JPROC.2014.2357031

current (dc) power [4], [5]. This concept of wireless power transfer requires no motion, pressure, or heat flows to generate power.

There are two main types of wireless energy transfer (WPT) and harvesting: near-field or far-field system. Near-field WPT systems utilize electric/magnetic induction or magnetic resonance to transfer power wirelessly and usually have a high transfer efficiency more than 80% within a wavelength from the source [6]–[8], and a relatively longer distance inductive WPT system has been reported [9]. Electromagnetic energy decays at a rate of 60 dB/decade in near-field region (distance $< 0.1\lambda 0$), thus this approach is suitable for short-range energy harvesting or power transfer systems [10]. The strongly coupled magnetic resonance (SCMR) method which utilizes a four-coil configuration has been studied recently due to its high power transfer efficiency and an enhanced range up to few meters. For the far-field WPT systems, the energy-harvesting devices utilize antennas to collect remotely radiated electromagnetic waves and diode/transistor-based circuitry, such as rectifiers and charge pumps, for the RF–dc conversion. Some reported far-field wireless energy-harvesting systems used a directive beamforming technique to known sources' directions in order to collect a larger amount of power [11]–[13], while other systems utilize almost isotropic antennas when the direction of the sources in not well known or is time varying, featuring effectively lower harvested power densities [14]–[16].

In this paper, the properties of widely utilized ambient energy sources, such as thermal, solar, wireless, and piezoelectric sources, are introduced. Their available energy density level in an ambient environment, the output power efficiencies, and values as well as their respective advantages and disadvantages are discussed in detail. Reported research efforts on the far-field ambient wireless energy-harvesting technologies for low-power standalone electronics are also discussed among the numerous energy-harvesting technologies. The feasibility of the ambient wireless energy-harvesting technology is verified through the powering up of practical low-power embedded electronic systems, such as a sensor platform or a microcontroller unit (MCU). An ambient wireless energy harvester operating at ultrahigh-frequency (UHF) digital TV frequency band [15] and a dual-band wireless energy harvester at the industrial–scientific–medical (ISM) band of 915 MHz and 2.45 GHz [17] are presented as design examples for harvesting far-field nondirective electromagnetic waves. Both presented wireless energy harvesters have successfully converted RF power to dc power when they are exposed to ultralow power densities of 1 μW/cm^2 or lower. Last, the near-field wireless energy harvester for wearable electronics is introduced.

II. AMBIENT RF ENERGY-HARVESTING TECHNOLOGY

A. Energy Sources in Ambient Environment

Numerous available renewable ambient energy sources exist in nature [18], [19]. Widely utilized ambient energy sources are summarized in Table 1. Solar power is one of the most commonly used sources, featuring high power [20]. It has high power density of 100 mW/cm^2 during daytime with about 30% of conversion efficiency [21]. A solar panel can also operate in a hybrid mode in conjunction with other types of energy source [22], [23]. The photovoltaic technology has been well developed over the last 60 years after the first silicon-based solar cell had been demonstrated in the 1950s

Table 1 Available Ambient Energy Sources

	Solar Energy[20]-[23]	Thermal Energy[25]	Ambient RF Energy[18][35]	Piezoelectric Energy	
				Vibration[27][28]	Push Button[29]
Power Density	100 mW/cm^2	60 μW/cm^2	0.0002 ~ 1 μW/cm^2	200 μW/cm^3	50 μJ/N
Output	0.5 V (single Si cell) 1.0 V (single a-Si cell)	-	3 ~ 4 V (Open circuit)	10 ~ 25 V	100 ~ 10000 V
Available Time	Day time (4 ~ 8 Hrs)	Continuous	Continuous	Activity dependent	Activity dependent
Weight	5 ~ 10 g	10 ~ 20 g	2 ~ 3 g	2 ~ 10 g	1 ~ 2 g
Pros	▪ Large amount of energy ▪ Well developed tech.	▪ Always available	▪ Antenna can be integrated onto frame ▪ Widely available	▪ Well developed tech. ▪ Light weight	▪ Well developed tech. ▪ Light weight ▪ Small volume
Cons	▪ Need large area ▪ Non-continuous ▪ Orientation issue	▪ Need large area ▪ Low power ▪ Rigid & brittle	▪ Distance dependent ▪ Depending on available power source	▪ Need large area ▪ Highly variable output	▪ Highly variable output ▪ Low conversion efficiency (high volt./low amps.)

and its physical (flexibility, durability, etc.) and electrical (efficiency, output voltage, etc.) properties keep improving [24]. The available amount of power is determined by the size of a solar panel and various values of voltage or current can be generated by adjusting its size. However, a solar panel requires a relatively large area to collect sufficient amounts of ambient solar power due to low conversion efficiency of 10%–40%, and its orientation is critical to collect solar power. It is also inefficient on a cloudy day or at night due to the lack of the source.

Thermal energy of the power source is also widely utilized. Electrical power is directly generated by exploiting the temperature difference in thermoelectric devices taking advantage of thermoelectric effects, such as the Seebeck effect or the Thomson effect [25]. In reverse way, the thermoelectric material generates a temperature difference when a voltage is applied. The thermoelectric effect may also be used as a temperature sensor besides its energy-harvesting applications. In general, a thermoelectric generator produces an energy density of about 20–60 μW/cm^2 when it utilizes the human body as the heat source at room temperature of 18 °C–25 °C [26]. Thermoelectric devices can operate continuously as far as there is a temperature difference or a heat flowing across them, while they are usually rigid and heavy compared to other energy-harvesting devices, such as solar cells. The thermoelectric energy-harvesting devices typically require relatively large form factors in terms of volume to generate useful amounts of power.

The piezoelectric effect generates electrical voltages or currents from mechanical strains, such as vibration or deformation. Typical piezoelectric-based energy harvesters keep creating power when there is a continuous mechanical motion, such as acoustic noises and wind, or they sporadically generate power for intermittent strains, such as human motion (walking, clicking a button, etc.). Typical output power density values of usual piezoelectric materials are around 250 μW/cm^3 but they can create more power when a motion or deformation is intense [27]. The piezoelectric energy harvesters or piezoelectric transducers are a well-developed technology, and numerous energy-harvesting modules of this type have been reported [28]. The volume of the piezoelectric power generators is relatively small and light compared to other energy-harvesting devices, because a small crystalline structure is able to generate power in these configurations. However, the output power of piezoelectric effect-based power generators has a large dynamic range when irregular motions, such as human motions, are utilized as the driving force. The generated power usually consists of high voltage and low current resulting in low conversion efficiency values, while necessitating the use of voltage regulation circuitry to protect from voltage overshoots [29].

Ambient RF energy has a relatively low energy density of 0.2 nW/cm^2–1 μW/cm^2 compared to other energy sources [18], [35]. However, a larger amount of total available power can be harvested by utilizing a high gain antenna. The available or existing ambient energy density of ambient RF and wireless sources keeps increasing due to the ever expanding wireless communication and broadcasting infrastructure, such as analog/digital TV, AM/FM radio, WiFi networks, and cellular networks. The ambient RF power density is usually higher in downtown urban areas and in the proximity of the power sources (e.g., TV towers) [35]. The RF energy-harvesting technologies could be especially useful in charging a battery or powering up electronics wirelessly in scenarios in which it is hard to replace the batteries of the deployed wireless networks (e.g., bridges, buildings). It is also useful when the wireless networks are deployed in difficult to access areas (e.g., chemical plants and aircraft), and they can operate at any time of the day and at any topology as far as there exists a minimal ambient power. Ambient RF energy-harvesting systems can be easily integrated with different types of antennas as well as with other harvesting technologies, such as the solar cells [22], [23]. It is more challenging due to very low-power-density values and the low RF–dc diode conversion efficiency values to utilize ambient RF power when power harvesters are far away (more than 6 km) from the wireless sources but the harvested RF power can be still utilized by appropriately optimizing the duty cycle of the system (typically below 6%–8%) [30]. The conversion efficiency of RF–dc conversion circuits, such as a charge pump or a rectifier, is about 10%–30% due to low input power levels (from −30 to −20 dBm) but the harvested RF power can generate about 1.8–4.0 V with a total converted power of about 100 μW. This power level is sufficient to operate battery-assisted sensors periodically for a long time (more than five years). The harvested RF power gets larger as the antenna gain and energy density of the ambient environment increase, since the RF–dc conversion efficiency is improved due to the increased input power to the rectifying circuit.

The general structure of a typical energy-harvesting-enabled wireless sensor platform is shown in Fig. 1. A converter or a transducer converts the ambient energy forms to dc power and stores the converted energy in energy storage devices, such as a battery or a super capacitor. A power management unit (PMU) optimizes the collected power level through matching and duty cycle optimization in a power-efficient way. The lifetime of the "main" power sources, such as a battery, can be extended by introducing energy-harvesting systems that effectively recharge periodically the main power source or function as an auxiliary source itself. The main power source can be also removed when there is a sufficient energy to drive the whole system for a truly standalone ("battery-less") autonomous operation.

B. Related Work

Numerous research efforts have been reported on far-field ambient RF energy harvesting, as listed in Table 2

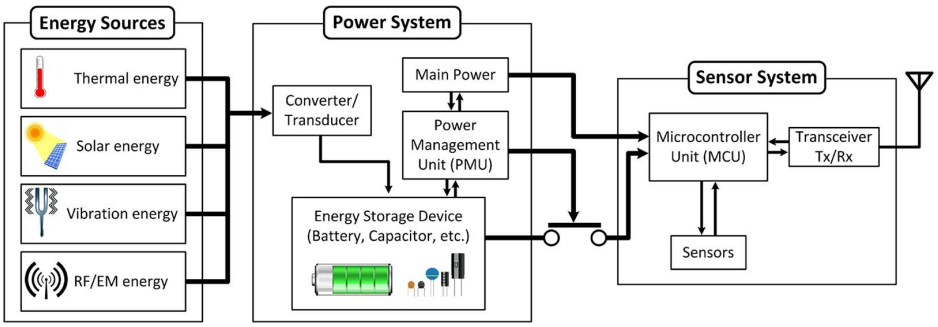

Fig. 1. ***General block diagram of an energy-harvesting-enabled wireless sensor platform system.***

[15], [30]–[36]. Radiated far-field power can propagate to a longer distance compared to near-field inductively coupled power due to a different attenuation rate. Far-field energy attenuates at 20 dB/decade, which is a much smaller rate compared to that of near-field energy [37]. Many reported efforts have used complementary metal–oxide–semiconductor (CMOS) technology to harvest power at UHF radio-frequency identification (RFID) band utilizing conventional RFID standards [38]–[41]. The RF energy harvesters based on CMOS technology are much more compact than board level designs, but they are challenging to optimize at various frequency bands and various input power levels once a design is fixed. In this section, recently reported board-level designs for far-field ambient RF energy harvesting are discussed.

Board-level harvesting systems utilizing the conventional RFID standards have been reported in [31] and [32], and have been optimized for collecting a single tone within the RFID frequency band of 862–928 MHz. They utilize an RFID reader as the source, which it has 2–4 W of

Table 2 Related Works

Related Work	RF Source	Sensitivity†	RF-DC Conversion Efficiency	Load*	Range	Tx Power
A. P. Sample *et al.* [31]	RFID Reader (915 MHz)	-8.7 dBm	30 %	180.0 kΩ Resistor	4.3 m	1 W
D. Donno *et al.*[32]	RFID Reader (866.5 MHz)	-14 dBm	16 %	3.0 kΩ Resistor	4.8 m	3.2 W (EIRP)
A. Dolgov *et al.* [33]	Ambient Cellular (1.96 GHz)	-15.2 dBm	60 %	1.0 kΩ Resistor	50 m	-
D. Masotti *et al.* [34]	Ambient Urban Wireless Signals: GSM900, and WiFi (900 MHz and 2.45 GHz)	-	~ 18 % (at -10 dBm)	50 Ω Resistor	1 m	50 mW
M. Pinuela *et al.* [35]	Ambient Urban Wireless Signals: Digital-TV, GSM900, GSM1800, and 3G (560 MHz, 900 MHz, 1.8 GHz, and 2.1 GHz)	-25 dBm	40 % (Overall)	100 µF Capacitor	-	-
T. Ajmal *et al.* [36]	Low Frequency Radio (909 kHz)	-	~ 50 %	1.0 kΩ Resistor	20 km	150 kW
R. J. Vyas et al. [15]	Ambient Digital-TV (512 ~ 566 MHz)	-14.6 dBm (Single tone) -37 dBm (Multi-tone)	15 %	100 µF Capacitor	6.3 km	48 kW (Atlanta)
R. Shigeta *et al.* [30]	Ambient Digital-TV (540 MHz)	-20 dBm	~ 30 % (at -10 dBm)	50 kΩ Resistor	6.3 km	380 kW (Tokyo)

†The required minimum received power to activate the system.
*The load connected to the output of the RF-DC convertor.

equivalent isotropic radiated power (EIRP) and operates in midrange (4–5 m). The sensitivity of the RFID-based RF energy-harvesting system has been improved to power values below −14 dBm by introducing a charge pump circuit; nevertheless, this sensitivity is not sufficient to harvest practical ambient wireless power from long-distance sources in TV, radio, or cellular bands.

Wireless energy-harvesting devices for ambient signals far away from the RF sources have been reported in [15], [30], and [33]–[36]. A rectifier with a dc–dc converter topology for the cellular frequency band at 1.96 GHz was proposed in [30]. The reported RF–dc conversion efficiency was more than 60% when the input power level was higher than −15 dBm (30 μW) and the RF source was 50 m away from the energy harvester, a shorter distance compared to other similar harvesters. A lithium battery was charged by the harvested RF power. The high density of RF energy in an urban area has been considered an energy source as well [34]–[36]. The wireless signals, such as TV, cellular, global system for mobile (GSM), and radio signals, are spread over multiple frequencies in urban areas although the power level of each signal could be as low as −40 dBm. Multiband antennas, optimized rectennas, and power management modules for each frequency band were designed and integrated to collect efficiently the ambient RF energy. A magnetic material loaded antenna was utilized to harvest energy in these reported efforts. The reported works in [33]–[36] demonstrated the feasibility of powering low-power electronics from prebuilt wireless infrastructure systems, such as a communication system or a broadcasting system, without a battery. Recently, an ambient digital TV signal at the UHF band has been harvested and autonomous operation of a sensor platform has been demonstrated in [15] and [30]. In this research effort, a high-gain broadband antenna was utilized to harvest a sufficient amount of power to turn on an embedded microcontroller or a sensor and implement a truly autonomous operability. Digital TV signals within 512–566-MHz frequency bands were captured, rectified, and stored in a capacitor to drive the embedded systems from 6.3 km away from the digital TV broadcasting station. A charge pump circuit was optimized to rectify and create 1.8–3.3 V from ambient RF power (below −25 dBm) at the UHF band.

III. COMMERCIAL PRODUCTS FOR ENERGY HARVESTING

There are several commercially available devices for ambient energy harvesting, as shown in Table 3. They are mostly integrated circuit (IC) designs for small form factor, and they utilize CMOS technology to minimize the quiescence current (I_Q). The definition of I_Q is the difference between the input currents and the output currents which is directly related to the conversion efficiency. Low quiescent or leakage current is especially important for harvesting the low-power-density energy sources, such as the RF and thermal energy sources, while the voltage/current regulation is a critical factor for the high-voltage or high-current energy sources, such as piezoelectric or solar power sources [27], [42]. Typically, each chip is optimized for a different ambient energy source/form but few lately reported chips are able to harvest energy from multiple sources, such as RF, thermal, and solar energy. In general, a device has high efficiency or low I_Q when it harvests energy from one or a small number of energy sources, such

Table 3 Commercial Energy-Harvesting Devices

Name	Manufacturer	Quiescence Current (I_Q)	Sensitivity	Output Voltage	Energy Source
[1]LTC3107	Linear Technology	80 nA (Harvesting) 60 µA (No harvesting)	20 mV	4.3 V	Thermal energy
[2]bq25505	Texas Instrument	325 nA	330 mV (Start-up) 100 mV (After start-up)	5.0 V	Solar energy, Thermal energy
[3]SPV1050	STMicroelectronics	-	180 mV	3.6 V	Solar and thermal energy
[4]MAX17710	MAXIM	625 nA	0.75 V	6.0 V	RF, solar, and thermal energy
[5]PCC110	Powercast	Peak efficiency: 75 %	-17 dBm	-	RF (100 MHz ~ 6 GHz)

[1]http://www.linear.com/product/LTC3107
[2]http://www.ti.com/product/bq25505
[3]http://www.st.com/web/catalog/sense_power/FM142/CL1810/SC1517/PF259832?icmp=spv1050_pron_pr-spv1050_dec2013
[4]http://www.maximintegrated.com/datasheet/index.mvp/id/7183
[5]http://www.powercastco.com/PDF/PCC110-PCC210-Overview.pdf

as Linear Technology's (Milpitas, CA, USA) LTC3107, which is designed to collect power only through the use of thermoelectric devices, but it features the lowest I_Q. Powercast's (Pittsburgh, PA, USA) PCC110 also has a high peak conversion efficiency of 75% as well as a good sensitivity of −17 dBm since it is optimized to harvest only from RF energy sources within the broadband range of 100 MHz–6 GHz. However, other devices (bq25505, SPV1050, and MAX17710) can harvest power from multiple energy sources, including solar, RF, and thermal energy to produce more power. For the purpose of design and development, a universal energy-harvesting evaluation kit, EnerChip energy processor (EP) universal energy-harvester evaluation kit (CBC-EVAL-09), was developed by Cymbet Corporation (Elk River, MN, USA) [43]. This kit is able to harvest multiple ambient energy sources, such as RF/EM, solar, thermal, and energy source, while having two internal 50-μAh solid state batteries in parallel as an energy storage device. Most off-the-shelf energy harvesters are utilizing a maximum power point tracking (MPPT) algorithm for high energy conversion efficiency and power monitoring [44]. The MPPT algorithms allow the energy-harvesting system to optimally deliver the collected power to a load or a storage device as well as maximize the power extraction from sources. Most of the commercially available energy-harvesting chips have been designed to be utilized as an auxiliary power source for wireless sensor networks (WSNs) or as a charger for a battery/capacitor to extend their lifetime. It is also feasible to construct a battery-free system for standalone sensors by utilizing such energy-harvesting devices.

However, the designed degree of freedom can be restricted when the commercially available energy-harvesting chips are utilized, although they are easier to use. The system performance characteristics, such as the operation frequency, the type of input energy sources, sensitivity, and loss, strongly depend on the specifications of an off-the-shelf chip, thus resulting in a limited system reconfiguration capability. The leakage or loss of the commercial energy-harvesting chips can be higher than the optimized board-level design due to prebuilt multisource energy-harvesting capabilities.

IV. EMBEDDED WIRELESS ENERGY-HARVESTER PROTOTYPE (E-WEHP)

Harvesting ambient RF energy and converting the harvested power to useful dc power requires a careful design. An optimized wireless power harvester for an UHF digital TV signal is shown in [15], and a block diagram of the proposed ambient RF energy-harvesting platform is shown in Fig. 2. The ambient RF power is captured by the antenna, and the charge pump converts the wireless power to usable dc power, which then charges the charge tank in order to operate the embedded MCU. The propagation loss

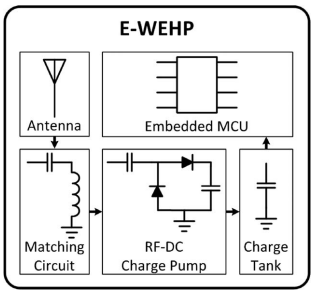

Fig. 2. *Block diagram of an embedded wireless energy-harvesting prototype (E-WEHP) [15].*

(L) of the radiated wave from the base station in decibels without wave diffraction can be expressed as

$$L = F + 18\log\left(\frac{17h + R^2}{17h}\right) \tag{1}$$

$$F = \left(\frac{4\pi R}{\lambda_0}\right)^2 \tag{2}$$

where F is the free space path loss, h is the height of the source, R is the distance from the RF source, and λ_0 is the wavelength [10]. The harvested dc power (P_{av}) of the RF energy harvester in decibels can be expressed as

$$P_{\mathrm{av}} = P_{\mathrm{Tx}} - L + G_{\mathrm{Rx}} + G_{\mathrm{Tx}} + \eta_{\mathrm{RF-dc}} \tag{3}$$

where P_{Tx} is the transmitted power of the source, G_{Rx} is the gain of the receive antenna, G_{Tx} is the gain of the transmitting antenna, and $\eta_{\mathrm{RF-dc}}$ is the efficient RF–dc conversion circuit. The height (h) and the transmitted power (P_{Tx}) of the source and the wavelength (λ_0) of the target band are typically fixed and cannot be manipulated by designers in practical ambient energy-harvesting systems. Thus, a high-gain antenna and an efficient RF–dc conversion circuit $(\eta_{\mathrm{RF-dc}})$ are necessary to achieve optimum energy-harvesting performance.

A. Ambient Power at UHF Band for Digital TV

As a proof of concept and without loss of generality, ambient E-field spectra between 50 and 800 MHz were measured in downtown Tokyo, Japan, and Atlanta, GA, USA, in daytime utilizing a NARDA SRM-3000 radiation meter [45], as shown in Fig. 3(a) and (b). The banded RF power density (S_{BA}) in London, U.K., is also shown as a comparison in Fig. 3(c) [35]. The base transmit band (BTx) and the mobile transmit band (MTx) are separated. Peak wireless power levels below the 100-MHz range were commonly observed due to FM radio broadcast in both cities. High radiation levels in the 100–500 MHz in Tokyo were due to analog TV broadcasts, while additional high radiation levels were observed commonly in 500–700 MHz due to digital TV broadcasts. The peak wireless power at the FM radio band is higher than digital TV, but its

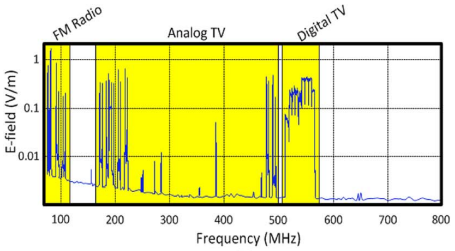

(a)

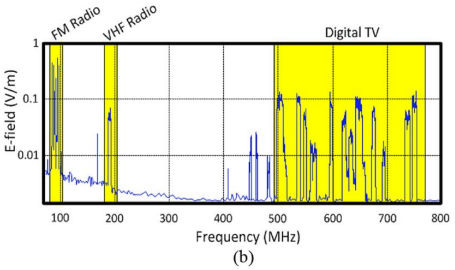

(b)

Band	Freq. (MHz)	Average S_{BA} (nW/cm^2)	Maximum S_{BA} (nW/cm^2)
DTV	470 ~ 610	0.89	460
GSM900 (MTx)	880 ~ 915	0.45	39
GSM900 (BTx)	925 ~ 960	36	1930
GSM1800 (MTx)	1710 ~ 1785	0.5	20
GSM1800 (MTx)	1805 ~ 1880	84	6390
3G (MTx)	1920 ~ 1980	0.46	66
3G (BTx)	2110 ~ 2170	12	240
WiFi	2400 ~ 2500	0.18	6

(c)

Fig. 3. *Ambient E-field intensity in (a) Tokyo, Japan and (b) Atlanta, GA, USA [15], and (c) RF power density in London, U.K. [35].*

channel bandwidth is narrower than the digital TV band resulting in a lower power density (power per channel bandwidth) that is available for harvesting over this frequency band. The digital TV band has multiple carriers to transmit larger amounts of data at 500–700-MHz band, resulting in higher net power over the frequency band than the FM radio band. It is also challenging to design a compact high-gain antenna at the FM radio band due to its physically long wavelength (about 3.3 m) while the antenna for the UHF digital TV band can be easily miniaturized to capture the wireless energy efficiently. The peak transmitting power of digital TV is 48 kW, while that of analog TV is 380 kW in measurements performed in Tokyo. However, the power density of digital TV signals is higher than analog TV due to its multicarrier broadcasting standard. Digital TV signals are also less affected by environmental objects or obstacles in urban areas, such as multipath interference, atmospheric noise, stray electromagnetic interference, and scattering [46], [47].

Digital TV uses a 6-MHz channel bandwidth to broadcast high-definition television (HDTV) signal which has 1920-by-1080-pixel video, and the digitally compressed high-resolution video and audio data are transmitted over multiple carriers within the 6-MHz channel bandwidth [46], [47]. The Integrated Services Digital Broadcasting Standard (ISDB-T) is utilized in parts of Asia, including Japan, and of South America for digital TV broadcasting. Each HDTV channel under ISDB-T uses 6-MHz-wide bandwidth between frequency band of 470 and 770 MHz, while including 5617 carriers at about 1-kHz frequency spacing. The Advanced Television System Committee Standard (ATSC), which uses a similar multicarrier method, has been used since 2009 for digital TV broadcasting in North America [48].

The ambient wireless power at the UHF digital TV band in Tokyo, Japan, captured by a broadband log-periodic antenna which had a realized gain of 7 dBi on average at the band, is shown in Fig. 4. The transmit antenna for digital TV was located 250 m above ground, and the distance between the digital TV antenna and the measurement site was 6.3 km. The Tokyo Metropolitan Television Broadcasting Corporation (JOMX; 512–518 MHz, Ch9) band transmitted power of 5 kW at the source and the measured power was 0.93 μW. Fuji Television Network, Inc. (JOCX; 518–524 MHz, Ch8), Tokyo Broadcasting System Television, Inc. (JORX; 524–530 MHz, Ch6), TV Tokyo Corporation (JOTX; 530–536 MHz, Ch7), TV Asahi Corporation (JOEX; 536–542 MHz, Ch5), Nippon Television Network Corporation (JOAX; 542–548 MHz, Ch4), NHK Educational TV (JOAB; 548–554 MHz, Ch2), and NHK General TV (JOAK; 554–MHz, Ch1) bands transmitted 48 kW at the source and the measured power was 11.7–29 μW. The Tokyo Tower (JOUD; 560–566 MHz, Ch12) band transmitted 19 kW at the source and the measured power was 3.73 μW.

B. Antenna for UHF Digital TV Signal Harvesting

A digital TV standard utilizes a linearly polarized wave parallel to the ground and a frequency band of 512–566 MHz [46]. The bandwidth of an antenna for an ambient UHF band wireless power harvester should cover the UHF digital TV frequency band. A high antenna gain is also required to harvest as much wireless power as possible, especially in the case when the source location/orientation is known. For the purpose of the proof of concept, a miniaturized log-periodic antenna was chosen because it features polarization matching, higher gain values than monopole/dipole antennas, and a wider bandwidth than Yagi–Uda antennas [49].

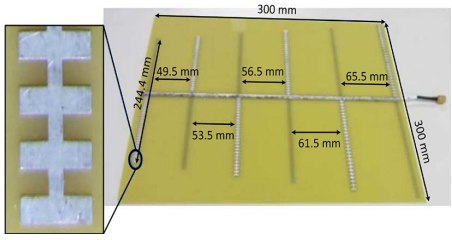

Fig. 4. *Fabricated log-periodic antenna on 1.6-mm-thick FR4 [15].*

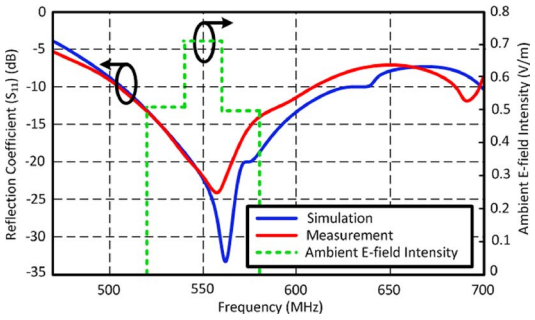

Fig. 5. *Simulated and measured reflection coefficients (S_{11}) and corresponding ambient E-field intensity of digital TV broadcasts in Tokyo, Japan [15].*

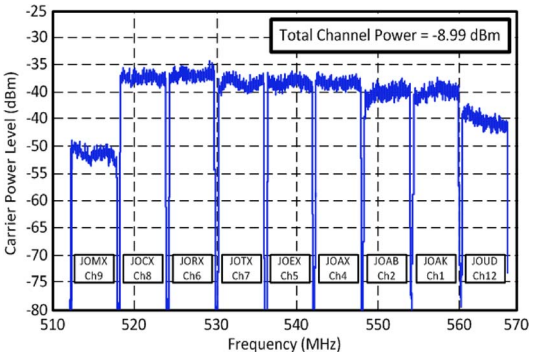

Fig. 7. *RF power captured by the E-WEHP log-periodic antenna (gain: 6–7 dBi) in Tokyo, Japan [15].*

A 3-D full-wave time-domain simulator, CST Microwave studio 2010, was used to design and optimize the proposed log-periodic antenna. The designed antenna on the 1.6-mm-thick FR4 board is shown in Fig. 4. Fishbone-shaped ridges were loaded to the dipole elements to miniaturize the log-periodic antenna by exciting slow waves while maintaining a relatively high antenna gain [50]. The optimized antenna geometry consisted of six elements with a scaling factor (τ) of 0.95, and the whole size of the proposed antenna was 300 mm $\times$ 300 mm. The measured reflection coefficient (S_{11}) matches the simulation results verifying the antenna's radiation performance over the desired UHF digital TV band of 512–566 MHz, as shown in Fig. 5, which also displays the measured ambient E-field intensity. The antenna gain values were measured in an anechoic chamber and are shown in Fig. 6. The simulated and measured gain showed good agreement, and an average gain value around 6.5 dBi (peak gain: 7.3 dBi at 540 MHz) at digital TV signal band was observed. The fabricated antenna prototype featured end-fire radiation patterns on E-plane and H-plane over the operation frequency band and a 3-dB beam width of 62.7° in E-plane. It should be noted that the designed antenna was optimized to have the best performance in terms of gain and reflection coefficient (S_{11}) at the frequency band of 540–560 MHz since the peak power density of the digital TV signal was observed at those frequencies. The measured peak carrier power level captured by the designed antenna at 6.3 km away from the source was -35 dBm (0.32 μW) while the net harvested wireless power was 126.2 μW (-8.99 dBm), as shown in Fig. 7.

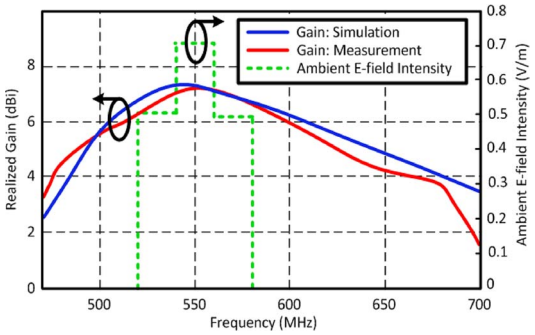

Fig. 6. *Simulated and measured realized antenna gains and corresponding ambient E-field intensity of digital TV broadcasts in Tokyo, Japan [15].*

C. RF–DC Charge Pump Design

The designed charge pump was optimized to convert sub-μW RF power to dc power as well as step up the output voltage. The five-stage charge pump was designed to produce more than 1.8 V at the output load, which consisted of a 100-μF low-leakage capacitor (C_L) in parallel with an MCU PIC24F [51], as shown in Fig. 8. The embedded MCU operates in multiple modes (power-up, sleep, and active) for typical sensing applications resulting in a

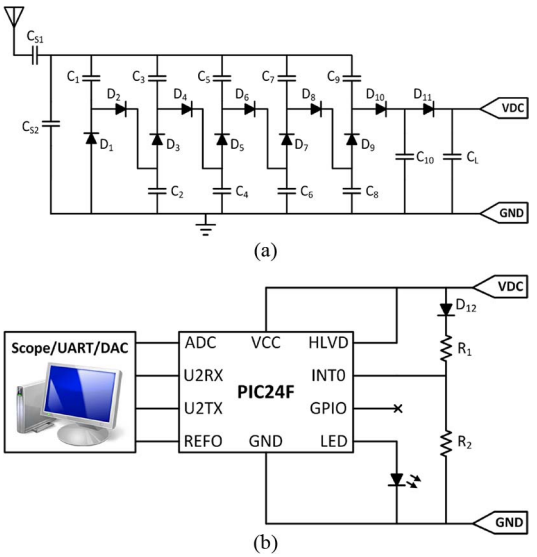

Fig. 8. *Circuit schematic E-WEHP: (a) charge pump and (b) MCU [15].*

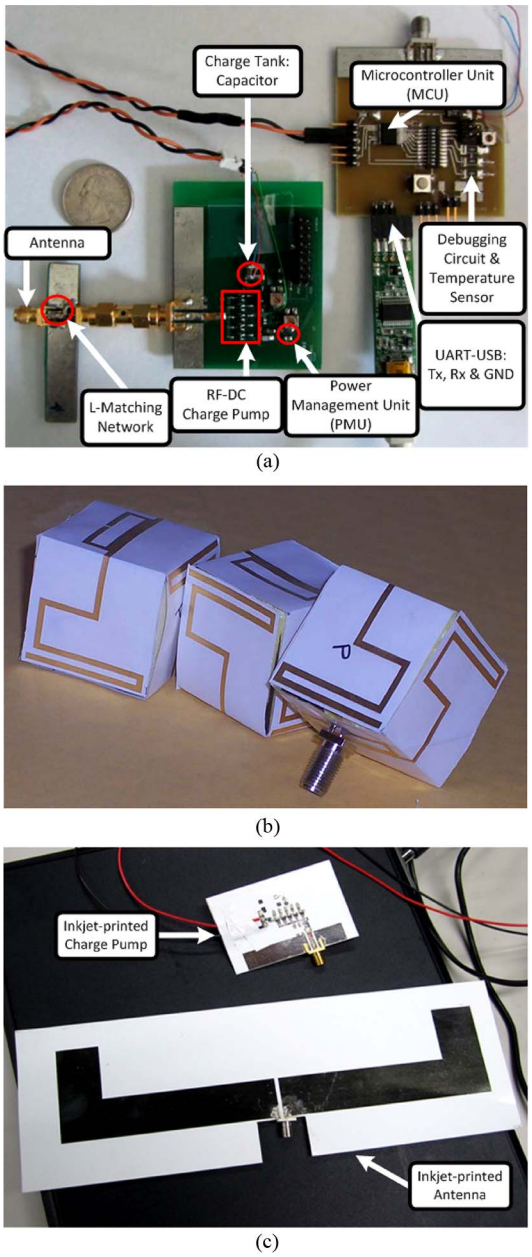

Fig. 9. ***(a) Fabricated prototype consisting of an RF–dc charge pump, embedded MCU, PMU, and sensor [15]. (b) Three-dimensional energy-harvesting "quasi-omnidirectional" antennas [53]. (c) Inkjet-printed prototype of the energy harvester on a paper substrate [54].***

time-varying load. The whole fabricated system is shown in Fig. 9(a).

The five-stage charge pump topology was chosen since three-stage to five-stage charge pumps yield the optimal output voltage for the low input power levels (below −15 dBm) while generating high voltage (> 1.8 V) enough to turn on the MCU [53]. The odd-numbered capacitors (C_1, C_3, C_5, C_7, and C_9) are charged to a voltage equal to the input RF voltage plus the voltage of the even-numbered capacitors through the odd-numbered diodes (D_1, D_3, D_5, D_7, and D_9) during the first half-cycle (the voltage across the input port is a positive value) of the input RF signal. In the same way, the even-numbered capacitors (C_2, C_4, C_6, C_8, and C_{10}) are charged through the even-numbered diodes (D_2, D_4, D_6, D_8, and D_{10}) during the next half-cycle (the voltage across the input port is a negative value) of the input RF signal. The rectified output voltage (V_{cap}) across the charge tank (C_L) can be calculated by

$$V_{\text{cap}} = 2xV_f - (2x+1)V_d \tag{4}$$

where x is the number of charge pump stages, V_f is the induced voltage due to the input RF signal, which can be calculated by the antenna gain value and the ambient power density, and V_d is the forward voltage drop of the diode. It is critical to select diodes which have a low forward voltage drop, such as the Schottky diodes, to maximize the harvested RF power as well as to keep the circuit size as small as possible to minimize substrate and conductor losses.

The RF–dc conversion efficiency can be estimated by

$$\eta_{\text{RF-dc}} = \frac{\text{delivered dc power to the load}}{\text{total input energy}} = \frac{C_L V_{\text{cap}}^2}{2P_{\text{in}}T_{\text{Vcap}}} \times 100 \tag{5}$$

where P_{in} is the input RF power and T_{Vcap} is the time to charge the charge tank to 1.8 V. The RF–dc conversion efficiency of the designed charge pump circuit which generates 1.8 V across the output loads of 1 and 18 MΩ in parallel with the 100-μF charge tank capacitor was also measured. Each resistor has the value of 1 and 18 MΩ representing the on- and off-states of the sensor, respectively. The maximum RF–dc conversion efficiency was 19.5% with 1-MΩ load while it was 21.0% with 18-MΩ load at an input power level of 330 μW (−4.74 dBm). The conversion efficiency at the input power level of 126 μW (−8.99 dBm), which is the net power level (total power from each channel) of digital TV band (512–566 MHz) at 6.3 km away from the TV broadcasting antennas, was 5.5% and 15.0% for 1- and 18-MΩ loads, respectively. Two types of L-matching network were designed for each input power due to the different input power levels. The matching network ensures the optimized operation at the UHF digital TV band, while the operation frequency of the diodes (Skyworks SMS7630 series) is from dc to 24 GHz.

D. Embedded Devices Powered by Ambient RF Power

One MCU was integrated with the designed charge pump circuit to implement a zero power autonomous sensor platform, as shown in Figs. 8 and 9(a). Recently, the

first ambient energy harvesters as well as the first fully 3-D energy-harvesting "quasi-omnidirectional" antennas [55] fabricated with additive manufacturing techniques (e.g., inkjet printing) [55], [56] have been reported for ultralow-cost substrate implementations [Fig. 9(b) and (c)]. Most of the off-the-shelf microcontrollers need 1.8–3.6 V to operate, which can be covered by the designed charge pump circuit [52], [55], [56]. Most microcontrollers also support the ultralow-power "sleep mode," which consumes only 20–650 nA with limited memory and peripheral usage, nevertheless, their power consumption is in the order of milliamperes (mA) at higher clock speed megahertz (MHz) or tens of microamperes (μA) at lower clock speed kilohertz (kHz) [51], [56], [57]. The designed E-WEHP utilized the Microchip's 16-b microcontroller PIC24F16-KA101 [51], which includes an analog-to-digital converter (ADC), a real-time clock and calendar (RTCC), and a high–low voltage detect (HLVD). The embedded MCU was successfully operated by limiting its duty cycle of the MCU utilizing the harvested RF power at the UHF digital TV band, which was stored at the charge tank. The harvested power was stored at the charge tank (100-μF capacitor) during the sleep mode (charge mode) of the MCU; after the charge tank power reached a sufficient value to drive the embedded components (e.g., sensor), the charge tank discharged the stored power (discharge mode). The PMU controls the operation modes of the MCU by monitoring the voltage of the charge tank capacitor.

The three operation modes (power-up, sleep, and active) of the MCU are listed in Table 4, and the operation algorithm is shown in Fig. 10. Most MCUs have a substantial amount of current leakage at inputs/outputs (Is/Os) because I/O pins are not biased at initial power-up mode. Numerous research efforts have been reported to handle this issue. In [33], the proposed energy harvester operates close to the RF source, and in [31], a battery was used to power up the device. The presented E-WEHP in this paper operates depending on an embedded software-based approach to power up the MCU at the initial stage utilizing the stored energy in the charge tank (100-μF capacitor) without a battery or an extensive power management hardware. The unavoidable power leakage during the power-up mode can be reduced by utilizing a faster clock. It takes about 1–10 ms to wake up the central processing unit (CPU) of the MCU (PIC24F) when it utilizes an 8-MHz startup clock, while a 32-kHz startup clock takes about 300 ms [51]. It has to be noted that a faster startup time reduces the discharging time of the charge tank during the power-up mode. Thus, the CPU clock speed was slowed down from 8 MHz (drains 2.25 mA) to 32 kHz (drains 8 μA) to minimize the power consumption after the power-up mode. As the last stage in the power-up mode, only RTCC and external interrupt (Ext INT) modules are turned on in order to monitor the voltage of the charge tank and the time stamping of the embedded sensors. In this way, the MCU can be powered up with low-power leakage in short time and put itself into a low-power sleep (charge) mode for an autonomous operation, as shown in Fig. 11(a) and (b).

In the sleep (charge) mode, the MCU is set to a deep sleep mode after power-up mode with only an RTCC module enabled. The MCU drains only 490–800 nA during this mode and maintains 1.9 V (Fig. 11). The MCU is waiting for an external interrupt (Ext INT) or sensor interrogation when it is in a sleep mode. The operation stages of the MCU are shown in Fig. 11. The charge tank needs about 66 s to charge from 1.9 to 3.75 V by harvesting

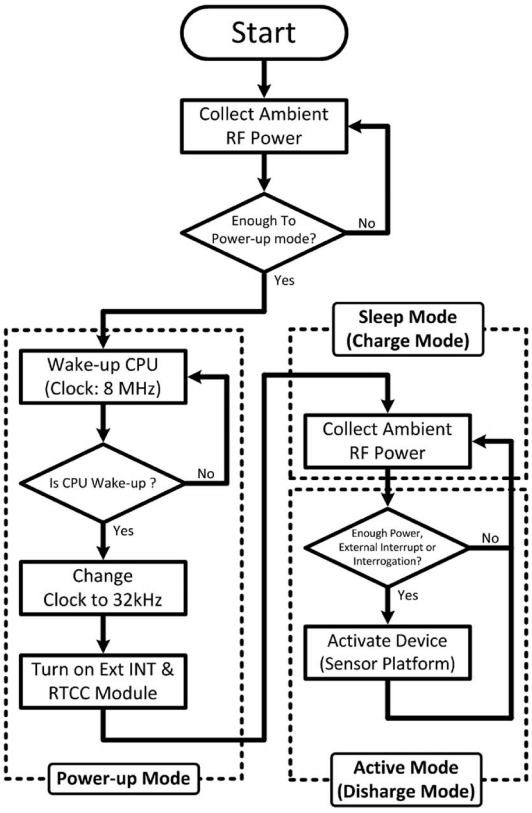

Fig. 10. ***Operation algorithm of the proposed ambient wireless energy harvester (E-WEHP).***

Table 4 Operation Modes of Embedded MCU

Operation Mode	CPU Clock Speed	MCU Peripherals
Power-up	8 MHz	-
Sleep (charge)	32 kHz	RTCC
Active (discharge)	32 kHz ~ 8 MHz	RTCC, ADC, UART[1], LED[2], Ext INT[3]

[1]UART: universal asynchronous receiver/transmitter, [2]LED: light emitting diode, [3]Ext INT: external interrupt.

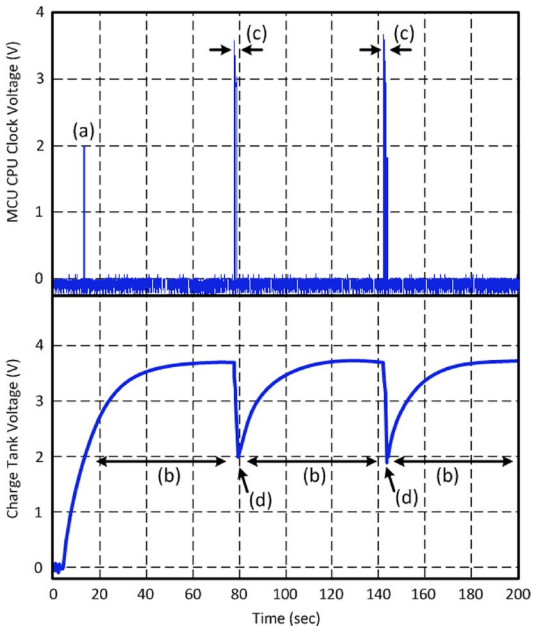

Fig. 11. *Operation of embedded MCU powered by ambient wireless power at the UHF digital TV band in Tokyo, Japan (channel power: −8.99 dBm): (a) power-up mode, (b) sleep/charge mode, (c) active/discharge mode, and (d) transition from active to charge mode [15].*

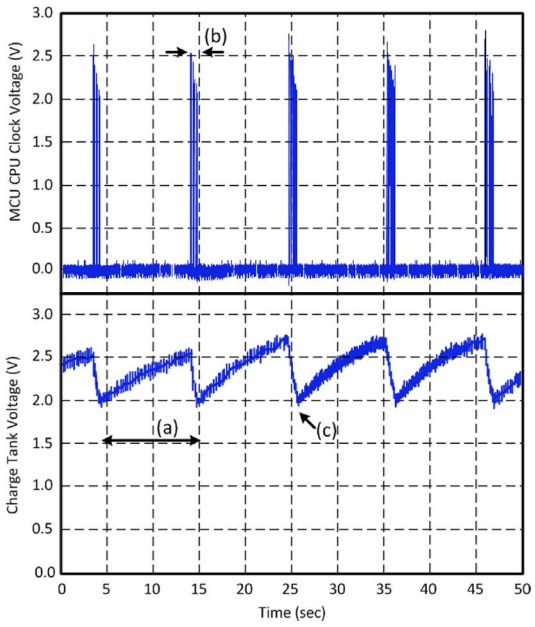

Fig. 12. *Operation of an embedded MCU, which is powered by ambient wireless power at the UHF digital TV band in Atlanta, GA, USA (channel power: −13.92 dBm): (a) sleep/charge mode, (b) active/discharge mode, and (c) transition from active to charge mode [15].*

ambient wireless power, as shown in Fig. 11(b). The operation voltages of 1.9 and 3.75 V were chosen since the operation voltage of the MCU is of 1.8–3.6 V. For demonstration purposes, the MCU was programmed to wake up every 60 s, because it took about 60 s to reach 3.6 V from 1.9 V. The MCU woke up periodically every 60 s and operated the clock, as shown in Fig. 11(c).

The peripheral modules of the MCU, such as the ADC and universal asynchronous receiver/transmitter (UART), are turned on in the "active (discharge) mode." It has to be stressed that the MCU needs to prevent the deep discharge of the charge tank during the active mode for an efficient autonomous operation utilizing the harvested ambient RF energy without the need of a battery. The deep discharge is regulated by D_{12}, R_1, and R_2 (Fig. 8). This regulation circuit cuts off the discharge when the voltage of the charge tank is lower than 1.8 V. The MCU interrupts the operation of the peripheral modules when it senses a high-to-low voltage transition and immediately returns to the "sleep mode," as shown in Fig. 11(d). A high forward voltage of D_{12} delays the leakage of the current from the charge tank through the resistors (R_1 and R_2) during the sleep mode. The measured consumed current during this regulation interrupt was 82.5 nA, which is much smaller than the current required for the operation of the MCU in the active mode. The operation time (T_{on}) of the MCU utilizing the harvested ambient wireless energy is a function of the charge tank capacitance (C_L), the available maximum voltage (V_{max}) by the charge pump, the turn-on voltage of the MCU (V_{MCU}), and the current (I_{MCU}) drawn by the MCU peripheral modules [15]. The observed cycle of the power-up mode, the sleep mode, the active mode, and voltage regulation is shown in Fig. 11.

The ambient UHF E-field measurement data in Atlanta, GA, USA, are shown in Fig. 3(b), and the performance data of a harvester of these power sources are shown in Fig. 12. North America uses the ATSC standard for the digital TV broadcasting, which has a lower net channel power as well as a lower carrier power level compared to Japan. The captured net channel power and the carrier power level through the optimized log-periodic antenna at 5.6 km away from the source was 40.55 μW (−13.92 dBm) and 64 nW (−42 dBm) from the source, respectively. The operation interval (duration of the sleep mode) was 10 s, as shown in Fig. 12. The duty cycle of the presented harvester in Japan was 3.3% while that of the harvester in Atlanta was 30%. The maximum voltage of the charge tank capacitor was to a lower value (2.7 V) in Atlanta due to the lower ambient power density, thus resulting in a larger measured duty cycle value.

The size of the proposed wireless energy harvester can be reduced by miniaturizing the antenna. The gain of the antenna decreases as the tradeoff of the antenna miniaturization, which results in less amount of the harvested power. It is necessary to adjust duty cycle of the battery-less sensor platform to compensate for the decreased harvested wireless power from the miniaturized antenna for the robust battery-less operation.

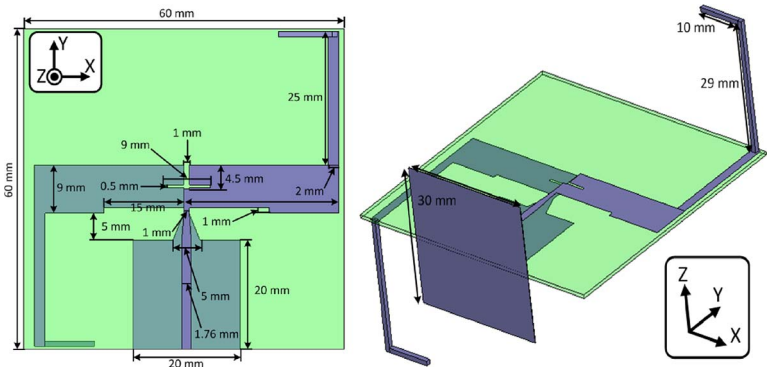

Fig. 13. *Geometry of the folded dipole antenna [17].*

V. DUAL-BAND CELL/WIRELESS ENERGY HARVESTER

A. Folded Dual-Band Antenna

A dual-band antenna at 915 MHz and 2.45 GHz was also designed to harvest RF power from cellular and WiFi sources with power densities around 1 μW/cm^2. The antenna geometry was a slot-loaded folded dipole antenna designed on 0.76-mm-thick Arlon 25N (ε_r: 3.38, $\tan\delta$: 0.0025), as shown in Fig. 13.

A half-wavelength-thick ($\lambda_0/2$) planar dipole antenna at 915 MHz was folded in order to miniaturize the size, and a slot was loaded in the middle of the antenna to add the second resonance at higher frequency of 2.45 GHz. A rectangular metal reflector was introduced to increase the antenna gain at each frequency band. The simulated and measured reflection coefficient values of the proposed antenna are shown in Fig. 14. The simulation and measurement match very well, and the bandwidth of the antenna covers both frequency bands around 915 MHz and 2.45 GHz.

The measured antenna gain at 915 MHz was 1.87 dBi and, at 2.45 GHz, it was 4.18 dBi. The harvested (received) power (P_r), which is input power to the rectifier at each frequency band, can be calculated using the measured gain (G), which is a dot product of the radiation efficiency (η_{eff}) and the directivity (D) and power density (ρRF) as

$$A_{\text{eff}} = \frac{\lambda_0^2}{4\pi}\eta_{\text{eff}}D = \frac{\lambda_0^2}{4\pi}G \tag{6}$$

$$P_r = \frac{\rho_{\text{RF}} \times A_{\text{eff}}}{\text{IL}} \tag{7}$$

where A_{eff} is the effective area of the antenna, and IL is the insertion loss factor of the matching networks.

The harvested (received) power is -8.81 dBm (131.52 μW) at 915 MHz and -15.05 dBm (31.26 μW) at 2.45 GHz. These values were utilized for the accurate design of the dual-band rectifier in Section V-B.

B. Dual-Band Rectenna

Fig. 15 shows the schematic of the dual-band rectifier, and Fig. 16 shows the fabricated rectenna. A single-stage rectifier was chosen in order to achieve low leakage and low insertion loss because the input power levels at each frequency band are very low (-9 dBm @ 915 MHz and -15 dBm @ 2.45 GHz) [1]. The single-stage rectifier is more efficient in this work because the load is a resistor different from the work in Section IV-C which has a capacitive load that needs a minimum voltage level of 1.8 V

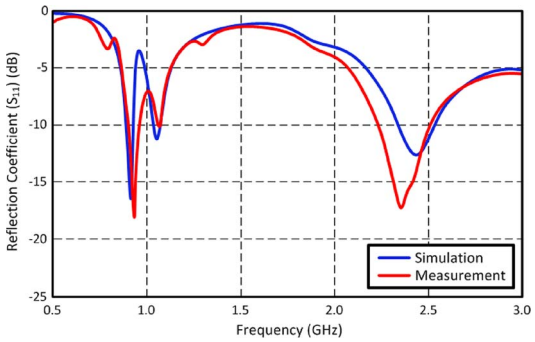

Fig. 14. *Reflection coefficient of the dual-band antenna [17].*

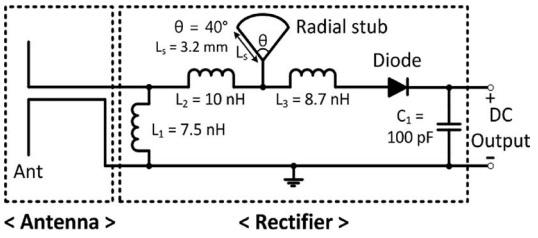

Fig. 15. *Schematic of the dual-band rectifier [17].*

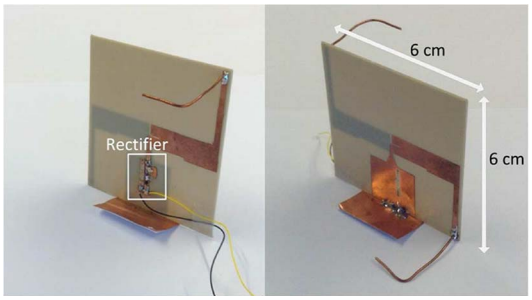

Fig. 16. *Fabricated dual-band rectenna prototype [17].*

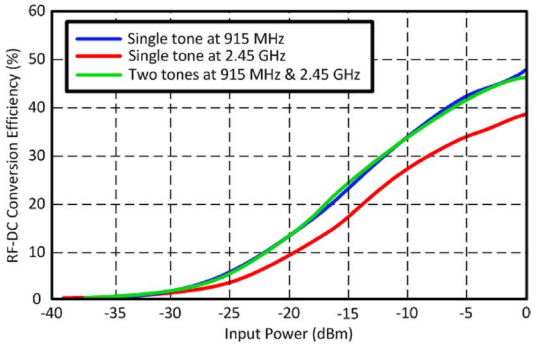

Fig. 18. *Measured RF–dc conversion efficiency for single- and dual-tone excitation [17].*

to turn on the MCU. A resistive load of 2.2 kΩ was connected to the rectifier to represent an integrated component, such as a sensor, and the input of the rectifier was matched to 50 Ω for an efficient antenna matching. In Section IV-C, the load resistance was in the order of MΩ because it represented the resistance of the I/O of the MCU, unlike the value of the load in this section, which represents a typical sensor component. The Skyworks SMS7630 Schottky diode was used for the design of the rectifier circuit.

The peaks of the simulated and measured reflection coefficient values (S_{11}) agree very well, as shown in Fig. 17. Single-tone and dual-tone signals were excited to measure the overall RF–dc conversion efficiency of the rectifier. Fig. 18 shows the measured conversion efficiencies depending on the input power levels and the number of tones. The RF input signals were summed up by a power combiner at the input of the rectifier. The conversion efficiency at 915 MHz with input power of −9 dBm was 37%, and the efficiency at 2.45 GHz with input power of −15 dBm was 20%. The measured harvested power of the rectenna at the power density of 1 μW/cm^2 was −13.88 dBm (40.91 μW) and −23.42 dBm (4.55 μW) at 915 MHz and 2.45 GHz, respectively.

The conversion efficiency of the proposed dual-band rectenna is relatively high compared to previously reported efforts, as shown in Fig. 19 [22], [58], [59]. In [22], a hybrid solar and wireless energy harvester was introduced. The reported hybrid device harvested solar and wireless power at the same time. An ultrawideband (UWB) antenna was used to harvest low RF power at multiple bands (850 MHz and 1.85 GHz), and the RF–dc conversion ratio was relatively low (8%–15%) due to the low-power density and to the low antenna gain, although a single-stage rectifier was utilized. In [58], a circularly polarized triple-band circular patch antenna was used to harvest power from ambient wireless sources. The commonly utilized resonator-type antennas feature relatively high-gain values resulting in large effective areas (A_{eff}), but they have narrow bandwidth and difficult-to-integrate feeding networks that maintain a circular polarization. In [58], a full-wave rectifier with a high RF–dc conversion ratio was reported because the power density of the ambient environment was relatively high (5 μW/cm^2) compared to other reported efforts. In [59], a planar triple-band antenna with a four-stage rectifier was introduced. The composite right/left hand (CRLH) transmission line concept was introduced to implement the planar triple-band antenna, and the four-stage rectifier was designed for triple-band

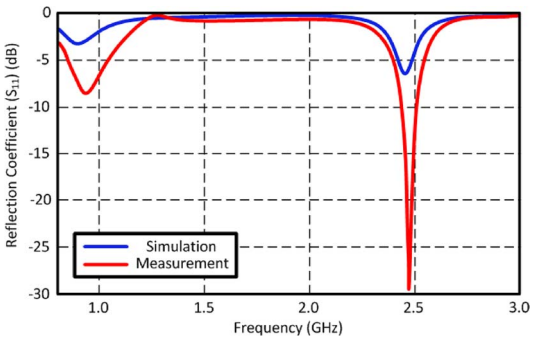

Fig. 17. *Reflection coefficient (S_{11}) of the dual-band rectifier [17].*

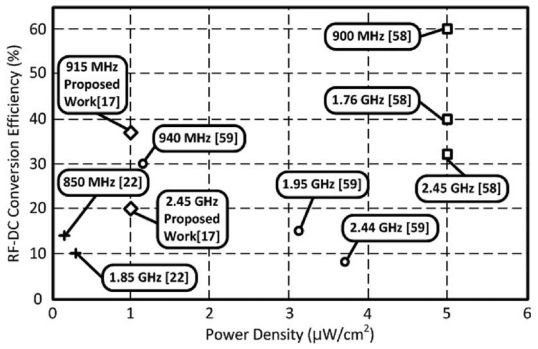

Fig. 19. *Multiband RF–dc conversion efficiency comparison [17].*

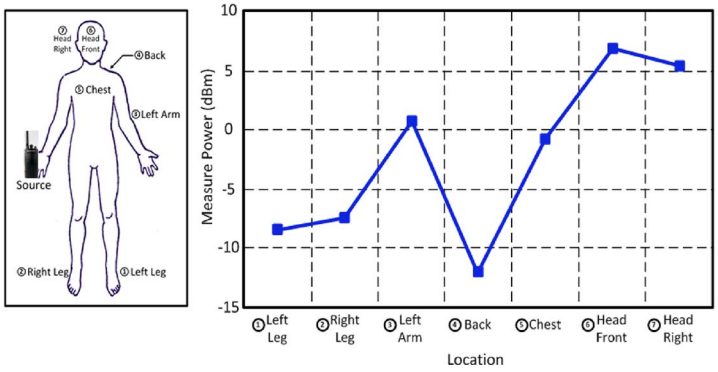

Fig. 20. ***Measured power levels around the human body for a commercially used two-way radio.***

matching, enabling an enhanced degree of freedom in design. However, this topology requires a high ambient power density or input power due to a relatively low antenna gain at each frequency as well as a high order of rectifier stages.

VI. NEAR-FIELD WIRELESS ENERGY HARVESTER FOR WEARABLE ELECTRONICS

A. Display and Power Source Characterization

As the use of wearable and implantable electronics and sensors is getting almost ubiquitous today, a wireless near-field energy harvester for an on-body display is discussed in this section [60]. The proposed system harvests the radiated signals from a commercially used two-way radio at the UHF band (464 and 468 MHz) as the power source to turn on/off an organic electrochromic display device. The display device changes its color from thick purple to transparent white when increasing the voltage difference across the display from 0 to 3 V. It typically takes about 2–4 s to change its color depending on the applied voltage. The display device can be modeled as a parallel resistor–capacitor (RC) tank based on measurements with the resistance and the capacitance values being equal to 100 Ω and 40 μF, respectively.

It is important to accurately assess the available ambient wireless power level around the human body for specific positions of the two-way radio in order to ensure the operation of the display powered by the RF energy harvester. To do that, commercial E-probes (ETS-Lundgren) were utilized to measure the available wireless power level. The probes were placed around the human body while the two-way radio was handheld in the right hand. The measured available wireless power levels are shown in Fig. 20. The two-way radio radiated 2 W of wireless power in a narrowband at 464 and 468 MHz. The lowest received power level was -12 dBm when the probe was placed on the back, while the measured maximum power level was 6.9 dBm when it was placed in front of the head. The distance between the source and the probe was about 0.5–1 m depending on the measuring position, while the transmitting power from the radio was kept at 2 W.

B. Folded Dipole Antenna and Rectifier Design

A folded dipole antenna was designed on a 1.57-mm-thick FR4 board to harvest power from the radio. The size of the designed antenna was 38 mm by 380 mm, and a 1 : 1 transformer, which served as a balun, was mounted at the input of the antenna for a balanced feeding. The size of the antenna can be miniaturized by meandering and folding the antenna geometry. The measured reflection coefficient (S_{11}) of the antenna with a balun is shown in Fig. 21. The calculated peak gain of the antenna was 3.2 dBi at 450 MHz with a high radiation efficiency value of 0.95, while featuring an omnidirectional radiation pattern.

A five-stage Dickinson RF–dc converter [Fig. 8(a)] was designed and integrated with the designed antenna through a matching circuit. The RF–dc converter with the matching circuit was optimized for power harvesting in the UHF band (400–500 MHz), and in combination

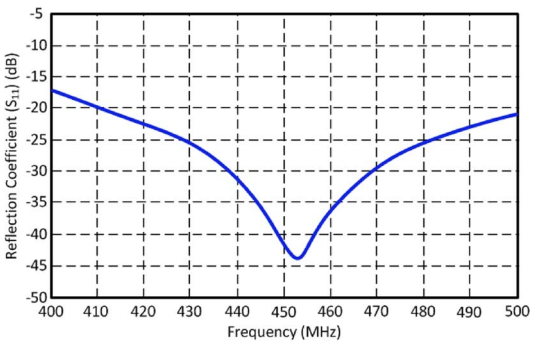

Fig. 21. ***Measured reflection coefficient (S_{11}) of the antenna [60].***

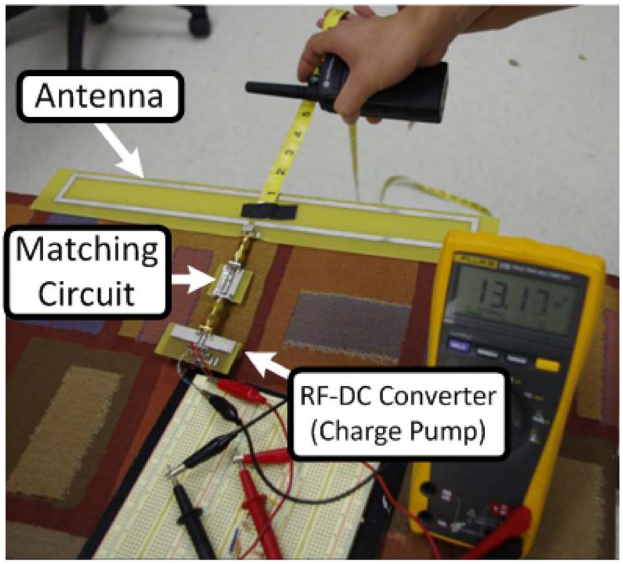

(a)

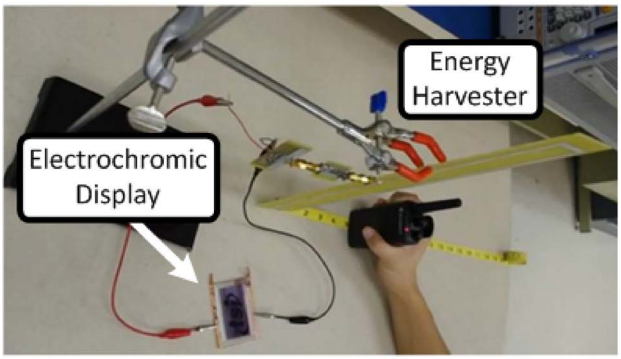

(b)

Fig. 22. ***System performance of the designed energy harvester with (a) a 1-M load and (b) the organic electrochromic display device [60].***

with the folded antenna, it generated up to about 1.7 V on the human body and 13 V in free space when the antenna was located at the Fresnel region (13 cm).

C. System Performance

The system performance of the designed power harvester was measured as shown in Fig. 22. The resistive load of a 1-MΩ resistor and the organic electrochromic display device were connected to the designed power harvester, respectively, while keeping the distance of 13 cm [Fresnel region, $\lambda_0/(2\pi)$] between the source and the harvesting device. A dc output voltage of 13.17 V was measured as shown in Fig. 22(a). The organic electrochromic device slowly changing the color from thick purple to transparent white by using the wireless power when it was integrated with the power harvester is shown in Fig. 22(b). The electrochomic device was successfully turned on when the folded dipole antenna was placed at the head front [⑥] and head right [⑦] positions.

VII. CONCLUSION

Ambient wireless energy-harvesting technologies have been thoroughly investigated in this paper for a variety of frequencies and power levels. The available average energy density of ambient wireless source is relatively lower than other energy sources, but the harvestable amount of power is sufficient to power up typical wireless sensor platforms and achieve self-sustainable operability by optimizing the duty cycle of the systems. The main advantage of ambient wireless power is its availability anytime/everywhere, which is a critical factor for the continuous operation of "zero-power" modules.

In the first prototype presented in this paper, the wireless power at the UHF digital TV band has been harvested through the use of a high-gain broadband antenna in order to operate a microcontroller-enabled sensor platform without a battery. This approach that is capable of harvesting low-power wireless signals at multiple channels resulted in a low threshold power (high sensitivity) to turn on the device. A highly efficient dual-band cell/WiFi energy harvester has been also presented with capability to collect larger amounts of power from multiple bands, while a single-stage rectifying circuit has been used to maximize an RF–dc conversion efficiency. Last, but not least, an optimized wireless energy harvester for on-body applications has been introduced and its performance has been verified through the activation of a wearable organic electrochromic device. All these examples have clearly demonstrated the significant capabilities of ambient wireless energy harvesting as an enabling technology for the first real-world self-sustainable implementations of Internet of Things, smart skin, smart city, and structural health monitoring configurations. ■

REFERENCES

[1] A. Boaventura, A. Collado, N. B. Carbalho, and A. Georgiadis, "Optimum behavior: Wireless power transmission system design through behavioral models and efficient synthesis techniques," *IEEE Microw. Mag.*, vol. 14, no. 2, pp. 26–35, Mar. 2013.

[2] Z. Popovic, E. A. Falkenstein, D. Costinett, and R. Zane, "Low-power far-field wireless powering for wireless sensors," *Proc. IEEE*, vol. 101, no. 6, pp. 1397–1409, Jun. 2013.

[3] R. Vyas *et al.*, "Paper-based RFID-enabled wireless platforms for sensing applications," *IEEE Trans. Microw. Theory Tech.*, vol. 57, no. 5, pp. 1370–1382, May 2009.

[4] W. C. Brown, "The history of power transmission by radio waves," *IEEE Trans. Microw. Theory Tech.*, vol. 32, no. 9, pp. 1230–1242, Sep. 1984.

[5] W. Lumpkins, "Nikola Tesla's dream realized," *IEEE Consum. Electron. Mag.*, vol. 3, no. 1, pp. 39–42, Jan. 2014.

[6] A. Kurs *et al.*, "Wireless power transfer via strongly coupled magnetic resonances," *Science*, vol. 317, no. 5834, pp. 83–86, Jun. 2007.

[7] H. Shoki, "Issues and initiatives for practical deployment of wireless power transfer technologies in Japan," *Proc. IEEE*, vol. 101, no. 6, pp. 1312–1320, Jun. 2013.

[8] M. Pinuela, D. C. Yates, S. Lucyszyn, and P. D. Mitcheson, "Maximising DC to load efficiency for inductive power transfer,"

IEEE Trans. Power Electron., vol. 28, no. 5, pp. 2437–2447, May 2013.

[9] J. Lawson, M. Pinuela, D. C. Yates, S. Lucyszyn, and P. D. Mitcheson, "Long range inductive power transfer system," *J. Phys., Conf. Ser.*, vol. 476, Dec. 2013, 012005.

[10] J. S. Seybold, *Introduction to RF Propagation*. New York, NY, USA: Wiley, 2005, pp. 134–162.

[11] Y. Fujino *et al.*, "A driving test of a small dc motor with a rectenna array," *IEICE Trans. Commun.*, vol. oE77-B, pp. 526–528, Apr. 1994.

[12] N. Shinohara and H. Matsumoto, "Experimental study of large rectenna array for microwave energy transmission," *IEEE Trans. Microw. Theory Tech.*, vol. 46, no. 3, pp. 261–268, Mar. 1998.

[13] L. Epp, A. Khan, H. Smith, and R. Smith, "A compact dual-polarized 8.51-GHz rectenna for high-voltage (50 V) actuator applications," *IEEE Trans. Microw. Theory Tech.*, vol. 48, no. 1, pp. 111–120, Jan. 2000.

[14] E. Falkenstein, M. Roberg, and Z. Popovic, "Low-power wireless power delivery," *IEEE Trans. Microw. Theory Tech.*, vol. 60, no. 7, pp. 2277–2286, Jul. 2012.

[15] R. J. Vyas, B. S. Cook, Y. Kawahara, and M. M. Tentzeris, "E-WEHP: A batteryless embedded sensor-platform wirelessly powered from ambient digital-TV signals," *IEEE Trans. Microw. Theory Tech.*, vol. 61, no. 6, pp. 2491–2505, Jun. 2013.

[16] H. J. Visser and R. J. M. Vullers, "RF energy harvesting and transport for wireless sensor network applications: Principles and requirements," *Proc. IEEE*, vol. 101, no. 6, pp. 1410–1423, Jun. 2013.

[17] K. Niotaki *et al.*, "A compact dual band rectenna using slot-loaded cual band folded dipole antenna," *IEEE Antennas Wireless Propag. Lett.*, vol. 12, pp. 1634–1637, May 2013.

[18] F. Yildiz, "Potential ambient energy-harvesting sources and techniques," *J. Technol. Studies*, vol. 35, no. 1, pp. 40–48. Fall, 2009.

[19] R. V. Prasad, S. Devasenapathy, V. S. Rao, and J. Vazifehdan, "Reincarnation in the ambiance: Devices and networks with energy harvesting," *IEEE Commun. Surv. Tut.*, vol. 16, no. 1, pp. 195–213, First Quarter, 2014.

[20] P. Jaffe and J. McSpadden, "Energy conversion and transmission modules for space solar power," *Proc. IEEE*, vol. 101, no. 6, pp. 1424–1437, Jun. 2013.

[21] M. A. Green, K. Emery, Y. Hishikawa, and W. Warta, "Solar cell efficiency tables (version 38)," *Progr. Photovoltaics, Res. Appl.*, vol. 19, pp. 565–572, Aug. 2011.

[22] A. Collado and A. Georgiadis, "Conformal hybrid solar and electromagnetic (EM) energy harvesting rectenna," *IEEE Trans. Circuits Syst. I, Reg. Papers*, vol. 60, no. 8, pp. 2225–2234, Aug. 2013.

[23] M. Danesh and J. R. Long, "Photovoltaic antennas for autonomous wireless systems," *IEEE Trans. Circuits Syst. II, Exp. Briefs*, vol. 58, no. 12, pp. 807–811, Nov. 2011.

[24] B. A. Gregg and M. C. Hanna, "Comparing organic to inorganic photovoltaic cells: Theory, experiment, simulation," *J. Appl. Phys.*, vol. 93, no. 6, pp. 3605–3614, Mar. 2003.

[25] G. Mahan, B. Sales, and J. Sharp, "Thermoelectric materials: New approaches to an old problem," *Phys. Today*, vol. 50, no. 3, pp. 42–47, Mar. 1997.

[26] V. Leonov, "Thermoelectric energy harvesting of human body heat for wearable sensors," *IEEE Sensors J.*, vol. 13, no. 6, pp. 2284–2291, Jun. 2013.

[27] H. S. Kim, J. -H. Kim, and J. Kim, "A review of piezoelectric energy harvesting based on vibration," *Int. J. Precision Eng. Manuf.*, vol. 12, no. 6, pp. 1129–1141, Dec. 2011.

[28] S. Roundy, P. K. Wright, and J. Rabaey, "A study of low level vibrations as a power source for wireless sensor nodes," *Comput. Commun.*, vol. 26, no. 11, pp. 1131–1144, Jul. 2003.

[29] G. Orecchini, L. Yang, M. M. Tentzeris, and L. Roselli, "Wearable battery-free active paper printed RFID tag with human-energy scavenger," in *IEEE MTT-S Int. Microw. Symp. Dig.*, Baltimore, MD, USA, Jun. 2011, DOI: 10.1109/MWSYM.2011.5973290.

[30] R. Shigeta *et al.*, "Ambient RF energy harvesting sensor device with capacitor-leakage-aware duty cycle control," *IEEE Sensors J.*, vol. 13, no. 8, pp. 2973–2983, Aug. 2013.

[31] A. P. Sample, D. J. Yeager, P. S. Powledge, A. V. Mamishev, and J. R. Smith, "Design of an RFID-based battery-free programmable sensing platform," *IEEE Trans. Instrum. Meas.*, vol. 57, no. 11, pp. 2608–2615, Nov. 2008.

[32] D. D. Donno, L. Catarinucci, and L. Tarricone, "An UHF RFID energy-harvesting system enhanced by a DC-DC charge pump in silicon-on-insulator technology," *IEEE Microw. Wireless Compon. Lett.*, vol. 23, no. 6, pp. 315–317, Jun. 2013.

[33] A. Dolgov, R. Zane, and Z. Popovic, "Power management system for online low power RF energy harvesting optimization," *IEEE Trans. Circuits Syst. I, Reg. Papers*, vol. 57, no. 7, pp. 1802–1811, Jul. 2010.

[34] D. Masotti, A. Costanzo, M. D. Preta, and V. Rizzoli, "Genetic-based design of a teta-band high-efficiency radio-frequency energy harvesting system," *IET Microw. Antennas Propag.*, vol. 7, no. 15, pp. 1254–1263, Dec. 2013.

[35] M. Pinuela, P. D. Mitcheson, and S. Lucyszyn, "Ambient RF energy harvesting in urban and semi-urban environment," *IEEE Trans. Microw. Theory Tech.*, vol. 61, no. 7, pp. 2715–2726, Jul. 2013.

[36] T. Ajmal, V. Dyo, B. Allen, D. Jazani, and I. Ivanov, "Design and optimisation of compact RF energy harvesting device for mart applications," *Electron. Lett.*, vol. 50, no. 2, pp. 111–113, Jan. 2014.

[37] K. Finkenzeller, *RFID Handbook*, 2nd ed. New York, NY, USA: Wiley, 2003, pp. 271–271.

[38] H. Reinisch *et al.*, "An electro-magnetic energy harvesting system with 190 nW idle mode power consumption for a BAW based wireless sensor node," *IEEE J. Solid-State Circuits*, vol. 46, no. 7, pp. 1728–1741, Jul. 2011.

[39] J. Yin *et al.*, "A system-on-chip EPC gen-2 passive UHF RFID tag with embedded temperature sensor," *IEEE J. Solid-State Circuits*, vol. 45, no. 11, pp. 2404–2420, Nov. 2010.

[40] D. Yeager *et al.*, "A 9μA, addressable Gen2 sensor tag for biosignal acquisition," *IEEE J. Solid-State Circuits*, vol. 45, no. 10, pp. 2198–2209, Oct. 2010.

[41] U. Karthaus and M. Fischer, "Fully integrated passive UHF RFID transponder IC with 16.7-W minimum RF input power," *IEEE J. Solid-State Circuits*, vol. 32, no. 10, pp. 1602–1608, Oct. 2003.

[42] F. Simjee and P. H. Chou, "Efficient charging of supercapacitors for extended lifetime of wireless sensor nodes," *IEEE Trans. Power Electron.*, vol. 23, no. 3, pp. 1526–1536, May 2008.

[43] Cymbet Corporation, "EnterChip EP universal energy harvesting eval kit," CBC-EVAL-09. [Online]. Available: http://www.cymbet.com/pdfs/DS-72-13.pdf

[44] V. Salas, E. Olias, A. Barrado, and A. Lazaro, "Review of the maximum power point tracking algorithms for stand-alone photovoltaic systems," *Solar Energy Mater. Solar Cells*, vol. 90, no. 11, pp. 1555–1578, Jul. 2006.

[45] NARDASRM 3000 Selective Radiation Meter Datasheet, Chicago, IL, USA, 2012. [Online]. Available: http://www.narda-sts.us/pdf_files/DataSheets/SRM3006_DataSheet.pdf

[46] D. Sparano, "What exactly is 8-VSB anyway?" ARRL, Newington, CT, USA, 1997. [Online]. Available: http://www.arrl.org/files/file/Technology/ TV_Channels/8_Bit_VSB.pdf

[47] NHK Japan Broadcasting Corporation, "Outline of the specification for ISDB-T," Tokyo, Japan, 1999. [Online]. Available: http://www.nhk.or.jp /strl/open99/de-2/shosai-e.html

[48] Agilent Technologies, "DTV ISDB OFDM project example," Santa Clara, CA, USA, 2005. [Online]. Available: http://cp.literature.agilent.com/litweb/pdf/ ads2005a/dtv/dtv124.html

[49] D. Isbell and R. Duhamel, "Broadband logarithmically periodic antenna structures," in *IRE Int. Conv. Rec.*, New York, NY, USA, Mar. 1957, pp. 119–128.

[50] B. S. Cook and A. Shamim, "Inkjet printing of novel wideband and high gain antennas on low-cost paper substrate," *IEEE Trans. Antennas Propag.*, vol. 60, no. 9, pp. 4148–4156, Sep. 2012.

[51] Microchip Technologies Inc., "PIC24F16KA102 family datasheet," Chandler, AZ, USA, 2009. [Online]. Available: http://ww1.microchip.com/downloads/ en/DeviceDoc/PIC24F16KA102_Family_datasheet_39927b.pdf

[52] G. D. Vita and G. Iannaccone, "Design criteria for the RF section of UHF and microwave passive RFID transponders," *IEEE Trans. Microw. Theory Tech.*, vol. 53, no. 9, pp. 2978–2990, Sep. 2005.

[53] C. M. Kruesi, R. J. Vyas, and M. M. Tentzeris, "Design and development of a novel 3D cubic antenna for wireless sensor networks (WSN's) and RFID applications," *IEEE Trans. Antennas Propag.*, vol. 57, no. 10, pp. 3293–3299, Oct. 2009.

[54] R. Vyas, V. Lakafosis, M. Tentzeris, H. Nishimoto, and Y. Kawahara, "A battery-less wireless mote for scavenging wireless power at UHF (470–570 MHz) frequencies," in *Proc. IEEE Int. Symp. Antennas Propag.*, Spokane, WA, USA, Jul. 3–8, 2011, pp. 1069–1072.

[55] L. Yang, A. Rida, R. Vyas, and M. M. Tentzeris, "RFID tag and RF structures on paper substrates using inkjet-printing technology," *IEEE Trans. Microw. Theory Tech.*, vol. 55, no. 12, pp. 2894–2901, Dec. 2007.

[56] Texas Instruments Inc., "TI MSP430F2274 mixed signal microcontroller datasheet," Dallas, TX, USA, Jul. 2011. [Online]. Available: www.ti.com

[57] Silicon Labs., "SiM3C1xx high-performance, low-power, 32-bit precision32 MCU family

with up to 256 kB of flash datasheet," Austin, TX, USA, 2012. [Online]. Available: http://www.silabs.com/Support%20Documents/TechnicalDocs/SiM3C1xx.pdf

[58] V. Rizzoli, G. Bichicchi, A. Costanzo, F. Donzelli, and D. Masotti, "CAD of multi-resonator rectenna for micro-power generation," in *Proc. EuMIC*, Rome, Italy, Sep. 28–29, 2009, pp. 331–334.

[59] B. L. Pham and A.-V. Pham, "Triple bands antenna and high efficiency rectifier design for RF energy harvesting at 900, 1900, and 2400 MHz," in *Proc. IEEE MTT-S Int. Microw. Symp.*, Seattle, WA, USA, Jun. 2–7, 2013, DOI: 10.1109/MWSYM.2013.6697364.

[60] R. Vyas, J. Bito, S. Kim, and M. Tentzeris, "Harvesting wireless signals from two-way talk-radios to power smart meters and displays," in *Proc. IEEE MTT-S Int. Microw. Symp.*, Tampa, FL, USA, Jun. 1–6, 2014, DOI: 10.1109/MWSYM.2014.6848669.

ABOUT THE AUTHORS

Sangkil Kim (Student Member, IEEE) received the B.S. degree in electrical and electronic engineering from Yonsei University, Seoul, Korea, in 2010 and the M.S. and Ph.D. degrees in electrical engineering from Georgia Institute of Technology, Atlanta, GA, USA, in 2012 and 2014, respectively.

He visited King Abdullah University of Science and Technology, Thuwal, Saudi Arabia, in 2013; Centre Tecnològic Telecomunicacions Catalunya (CTTC), Barcelona, Spain, in 2013; and CNRS-LAAS, Toulous, France, in 2013; as a visiting scholar. He is currently working on the design and fabrication of printed RF energy-harvesting-enabled standalone low-power sensor platform.

Rushi Vyas (Member, IEEE) received the B.Sc., M.Sc., and Ph.D. degrees in electrical and computer engineering from Georgia Institute of Technology, Atlanta, GA, USA.

He is currently an Assistant Professor in the Schulich School of Engineering, and a Researcher with the Pipeline Engineering Center (PEC), University of Calgary, Calgary, AB, Canada. His work has been covered in over 27 research publications in peer-reviewed journals and conference proceedings, and three book chapters covering topics in ambient RF energy harvesting, inkjet-printed electronics, wireless gas and structural-health sensors, and real-time-localization systems (RTLS). Prior to joining academia, he worked on cellular radios at Apple Inc. and Blackberry.

Prof. Vyas received finalist and honorable-mention awards at the 2008 and 2012 IEEE International Microwave Symposia and the 2008 and 2009 IEEE Antennas and Propagation Society International Symposia (APS). His work on RF-energy harvesting and battery-less sensors has also been covered in media forums such as *MSN News*, *Engadget*, *IEEE Institute*, *Energy Harvesting Journal*, and *New Energy and Fuel*.

Jo Bito received the B.S. degree in electrical and electronic engineering from Okayama University, Okayama, Japan, in 2013. He is currently working toward the Ph.D. degree in electrical and computer engineering at Georgia Institute of Technology, Atlanta, GA, USA.

He is a Research Assistant of ATHENA lab, Georgia Institute of Technology. His research interests include application of inkjet-printing technology for RF energy harvesting and the wireless power transfer technology for biomedical application.

Kyriaki Niotaki (Student Member, IEEE) was born in Crete, Greece. She received the B.S. degree in informatics and the M.S. degree in electronic physics with specialization in electronic telecommunication technology from Aristotle University of Thessaloniki, Thessaloniki, Greece, in 2009 and 2011, respectively. Currently, she is working toward the Ph.D. degree in the Signal Theory and Communications Department, Technical University of Catalonia (UPC), Barcelona, Spain.

Since December 2011, she has been with the Centre Tecnologic de Telecomunicacions de Catalunya (CTTC), Barcelona, Spain, as a Research Assistant. Her main research interests include energy-harvesting solutions and the design of power amplifiers.

Ms. Niotaki was the recipient of the IEEE Microwave Theory and Techniques Society (IEEE MTT-S) Graduate Fellowship Award in 2014.

Ana Collado (Senior Member, IEEE) received the M.Sc. and Ph.D. degrees in telecommunications engineering from the University of Cantabria, Cantabria, Spain, in 2002 and 2007, respectively.

She is currently a Senior Research Associate and the Project Management Coordinator at the Technological Telecommunications Center of Catalonia (CTTC), Barcelona, Spain, where she performs her professional activities. Her professional interests include active antennas, substrate integrated waveguide structures, nonlinear circuit design, and energy-harvesting and wireless power transmission (WPT) solutions for self-sustainable and energy-efficient systems. She has participated in several national and international research projects and has coauthored over 70 papers in journals and conferences. Among her activities she has collaborated in the organization of several international workshops in different countries of the European Union and also a Training School for PhD students. She was a Marie Curie Fellow of the FP7 project Symbiotic Wireless Autonomous Powered system (SWAP).

Dr. Collado serves on the Editorial Board of the *Radioengineering Journal*, and she is currently an Associate Editor of the IEEE Microwave Magazine and a member of IEEE MTT-26 Wireless Energy Transfer and Conversion and MTT-24 RFID Technologies.

Apostolos Georgiadis (Senior Member, IEEE) was born in Thessaloniki, Greece. He received the B.S. degree in physics and the M.S. degree in telecommunications from the Aristotle University of Thessaloniki, Thessaloniki, Greece, in 1993 and 1996, respectively, and the Ph.D. degree in electrical engineering from the University of Massachusetts at Amherst, Amherst, MA, USA, in 2002.

In 1995, he spent a semester with Radio Antenna Communications (RAC), Milan Italy. In 2000, he spent three months with Telaxis Communications, South Deerfield, MA, USA. In 2002, he joined Global Communications Devices (GCD), North Andover, MA, USA, where he was a Systems Engineer involved with CMOS transceivers for wireless network applications. In June 2003, he was with Bermai Inc., Minnetonka, MN, USA, where he was an RF/Analog Systems Architect. In 2005, he joined the University of Cantabria, Cantabria, Spain, as a Researcher. He is currently a Senior Research Associate and Group Leader of the Microwave Systems and Nanotechnology Department at the Centre Tecnològic de Telecomunicacions de Catalunya (CTTC), Barcelona, Spain, in the area of communications subsystems where he is involved in active antennas and antenna arrays and more recently with RFID technology and energy harvesting.

Dr. Georgiadis was the recipient of the 1996 Fulbright Scholarship for graduate studies with the University of Massachusetts at Amherst; the 1997 and 1998 Outstanding Teaching Assistant Award presented by the University of Massachusetts at Amherst; the 1999 and 2000 Eugene M.

Isenberg Award presented by the Isenberg School of Management, University of Massachusetts at Amherst; and the 2004 Juan de la Cierva Fellowship presented by the Spanish Ministry of Education and Science. He is involved in a number of technical program committees and serves as a reviewer for several journals including the IEEE TRANSACTIONS ON ANTENNAS AND PROPAGATION and the IEEE TRANSACTIONS ON MICROWAVE THEORY AND TECHNIQUES. He was the corecipient of the EUCAP 2010 Best Student Paper Award and the ACES 2010 Second Best Student Paper Award. He was the Chairman of COST Action IC0803, RF/Microwave communication subsystems for emerging wireless technologies (RFCSET) and the Coordinator of Marie Curie Industry-Academia Pathways and Partnerships project Symbiotic Wireless Autonomous Powered system (SWAP). He is a member of IEEE MTT-S TC-24 RFID Technologies (Chair 2012-2014) and IEEE MTT-S TC-26 Wireless Energy Transfer and Conversion. He serves on the Editorial Board of the *Radioengineering Journal* and as an Associate Editor of the IEEE MICROWAVE AND WIRELESS COMPONENTS LETTERS and *IET Microwaves, Antennas, and Propagation*. He is the Editor-in-Chief of the *Wireless Power Transfer* journal.

Manos M. Tentzeris (Fellow, IEEE) received the Diploma degree in electrical and computer engineering (magna cum laude) from the National Technical University of Athens, Athens, Greece and the M.S. and Ph.D. degrees in electrical engineering and computer science from the University of Michigan, Ann Arbor, MI, USA.

He is currently a Professor at the School of Electrical and Computer Engineering, Georgia Institute of Technology, Atlanta, GA, USA. He has published more than 500 papers in refereed journals and conference proceedings, five books, and 19 book chapters. He has helped develop academic programs in highly integrated/multilayer packaging for RF and wireless applications using ceramic and organic flexible materials, paper-based RFIDs and sensors, biosensors, wearable electronics, inkjet-printed electronics, green electronics and power scavenging, nanotechnology applications in RF, microwave MEMs, SOP-integrated (UWB, multiband, millimeter-wave, conformal) antennas and heads the ATHENA research group (20 researchers). He is currently the Head of the GT-ECE Electromagnetics Technical Interest Group, and he has served as the Georgia Electronic Design Center Associate Director for RFID/Sensors research from 2006 to 2010 and as the Georgia Tech NSF-Packaging Research Center Associate Director for RF Research and the RF Alliance Leader from 2003 to 2006. He was a Visiting Professor with the Technical University of Munich, Germany, during summer 2002; a Visiting Professor with GTRI-Ireland, Athlone, Ireland, during summer 2009; and a Visiting Professor with LAAS-CNRS, Toulouse, France, during summer 2010.

Dr. Tentzeris was the recipient/corecipient of the 2014 Georgia Tech ECE Distinguished Faculty Achievement Award; the 2013 IET Microwaves, Antennas and Propagation Premium Award; the 2012 FiDiPro Award in Finland; the iCMG Architecture Award of Excellence; the 2010 IEEE Antennas and Propagation Society Piergiorgio L. E. Uslenghi Letters Prize Paper Award; the 2011 International Workshop on Structural Health Monitoring Best Student Paper Award; the 2010 Georgia Tech Senior Faculty Outstanding Undergraduate Research Mentor Award; the 2009 IEEE TRANSACTIONS ON COMPONENTS AND PACKAGING TECHNOLOGIES Best Paper Award; the 2009 E.T.S. Walton Award from the Irish Science Foundation; the 2007 IEEE APS Symposium Best Student Paper Award; the 2007 IEEE IMS Third Best Student Paper Award; the 2007 ISAP 2007 Poster Presentation Award; the 2006 IEEE MTT Outstanding Young Engineer Award; the 2006 Asian-Pacific Microwave Conference Award; the 2004 IEEE TRANSACTIONS ON ADVANCED PACKAGING Commendable Paper Award; the 2003 NASA Godfrey Art Anzic Collaborative Distinguished Publication Award; the 2003 IBC International Educator of the Year Award; the 2003 IEEE CPMT Outstanding Young Engineer Award; the 2002 International Conference on Microwave and Millimeter-Wave Technology Best Paper Award (Beijing, China); the 2002 Georgia Tech-ECE Outstanding Junior Faculty Award; the 2001 ACES Conference Best Paper Award; the 2000 NSF CAREER Award; and the 1997 Best Paper Award of the International Hybrid Microelectronics and Packaging Society. He was the TPC Chair for the IEEE IMS 2008 Symposium and the Chair of the 2005 IEEE CEM-TD Workshop, and he is the Vice-Chair of the RF Technical Committee (TC16) of the IEEE CPMT Society. He is the Founder and Chair of the RFID Technical Committee (TC24) of the IEEE MTT Society and the Secretary/Treasurer of the IEEE C-RFID. He is the Associate Editor of the IEEE TRANSACTIONS ON MICROWAVE THEORY AND TECHNIQUES, the IEEE TRANSACTIONS ON ADVANCED PACKAGING, and the *International Journal on Antennas and Propagation*. He has given more than 100 invited talks to various universities and companies all over the world. He is a member of URSI-Commission D, a member of MTT-15 committee, an Associate Member of EuMA, a Fellow of the Electromagnetic Academy, and a member of the Technical Chamber of Greece. He served as one of the IEEE MTT-S Distinguished Microwave Lecturers from 2010 to 2012.